U.S. Department of Energy

HelioCon

Heliostat Consortium for
Concentrating Solar-Thermal Power

Analysis of Wind and Load Variations in a Full-Scale Operational Heliostat Field

SPIE Optics and Photonics Conference, 25 August 2026

Matthew Emes, Ulrike Egerer, Scott Dana, David Jager, Shashank Yellapantula

conceptional design • components • integration • mass production • heliostat field

Introduction

- Limited public data on wind-driven loads on heliostats in operational concentrating solar power/thermal (CSP/CST) central receiver plants
- Field measurement data in full-scale operating plants are useful and necessary to quantify:
  - Localized wind speed and turbulence variations within arrays for operating and stow load cases
  - Wind effects on structural loads and facet deformations
  - Optical errors and spillage losses for heliostat structural design and field performance model assessment

Photos by Scott Dana, NLR

Objectives

- Characterize wind and turbulence profiles and wind-driven structural loads on heliostats in the two outermost rows at the northwestern field edge and one heliostat in the interior of the field
- Analyze the load distributions and acceleration spectra on three instrumented heliostats in operating and stow positions
- Compare non-dimensional load coefficients for northerly (prevailing) and southerly (far-field) wind periods with ABLRF field measurements and scale model heliostats in wind tunnel experiments

Methodology – Field Measurements

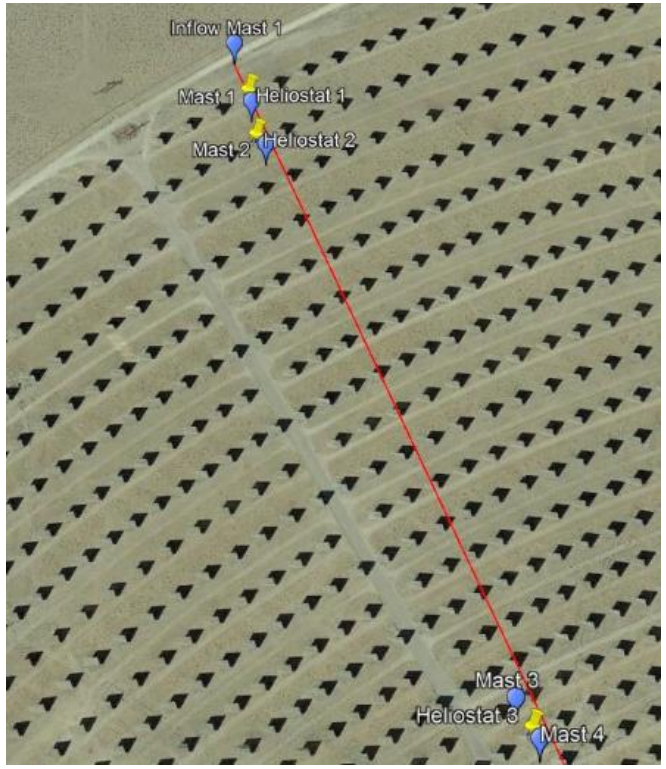

Image from Google Earth
© 2025 Google, Map Data © 2025 Airbus

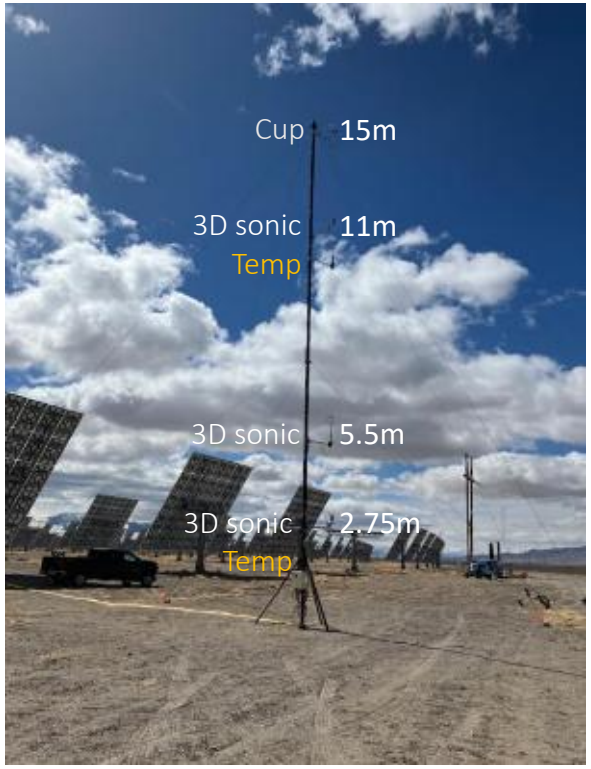

Photo by David Jager, NLR

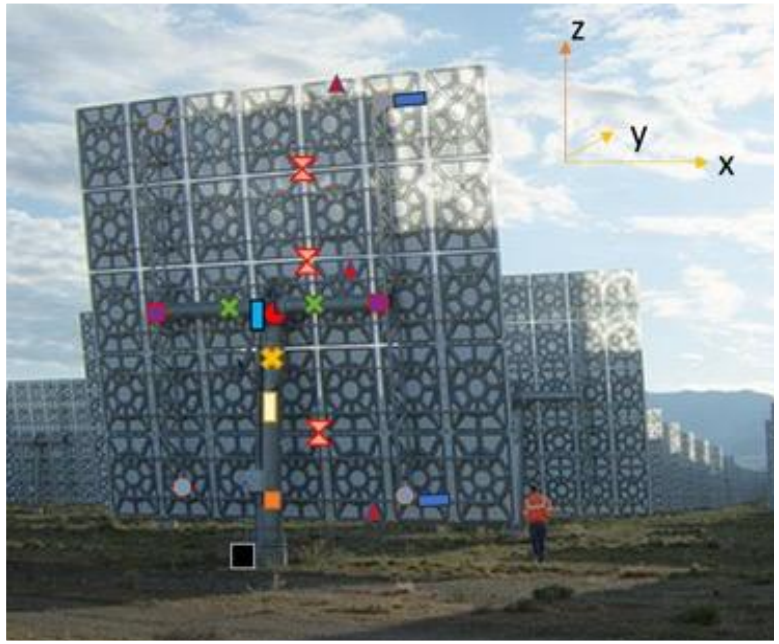

Photo by Scott Dana, NLR

- Pedestal bending strain gage
- Torque tube torque strain gage
- Pedestal torque strain gage
- Pedestal axial strain gage for lift forces
- Accelerometers on facet support structure
- Mirror facet laser displacement sensor
- Dynamic tilt inclinometer
- Support frame bending strain gage
- Differential pressure sensor between facets

Methodology – Data Postprocessing

- Met mast data – 3D sonic wind components and temperature processed to derive turbulence parameters and fluxes using signal processing and time correlation techniques
- Loads data – calculate strain gage slopes (kN/V/V and kNm/V/V) from component geometry and low-wind offsets compensated for variations in:
  - Elevation angle (gravity)
  - Temperature
- Low-wind (<2 m/s) periods from October 5 to December 12, 2024 for 1-min resampled load data
  - Elevation angle bin-averaged in 5° intervals from 5° to 85°
  - Temperature bin-averaged in 5°C intervals from -15°C to 30°C

https://data.openei.org/submissions/8601

Results – Wind Roses and Time Series

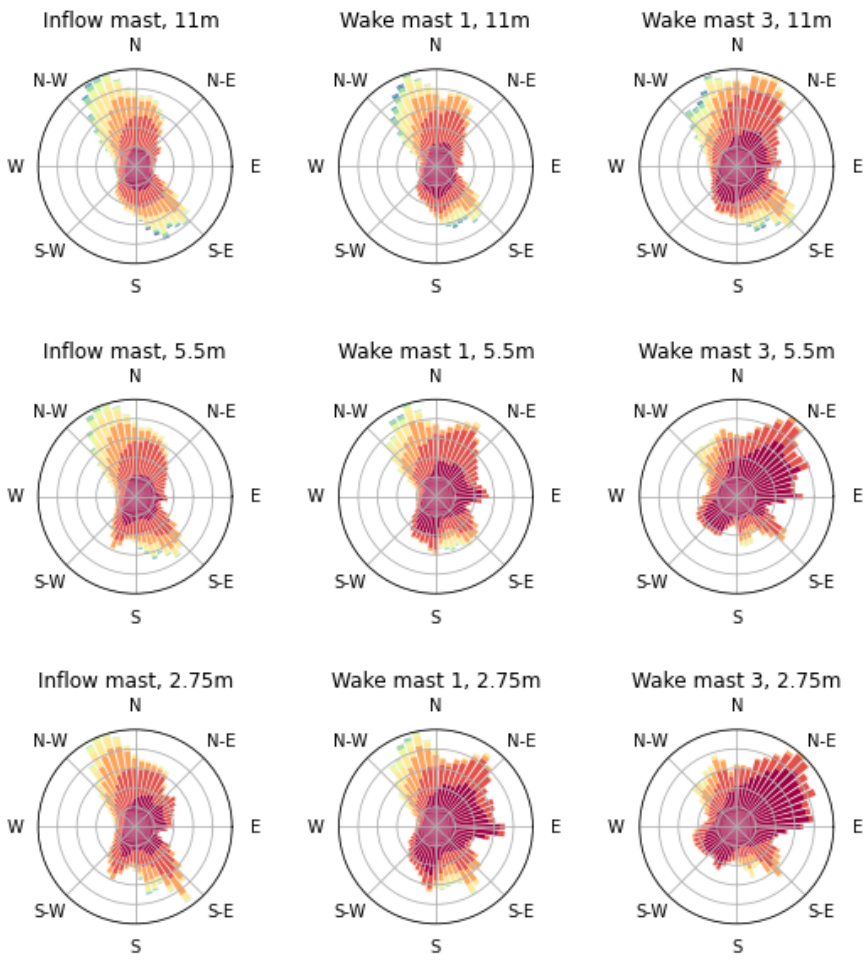

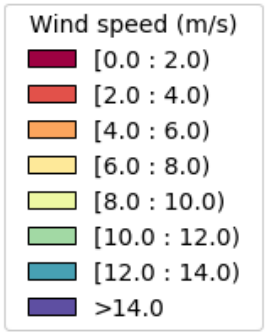

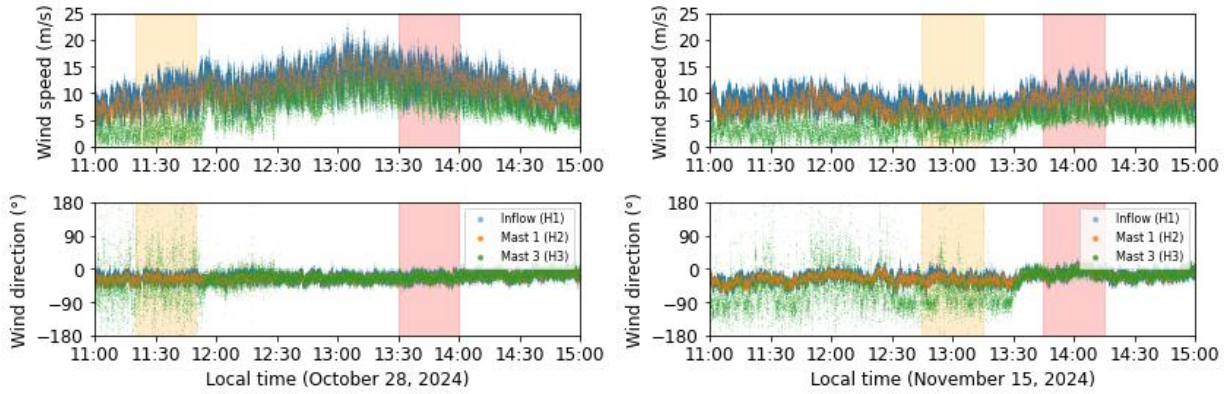

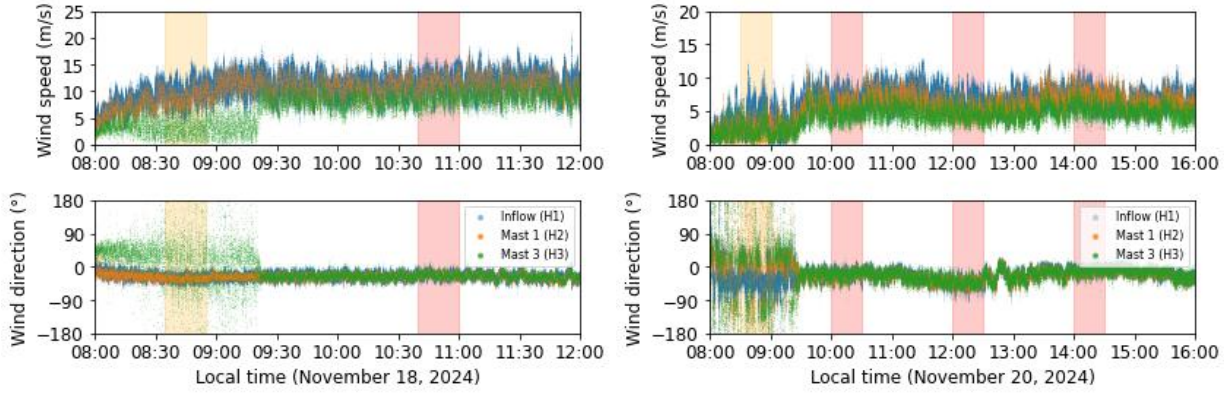

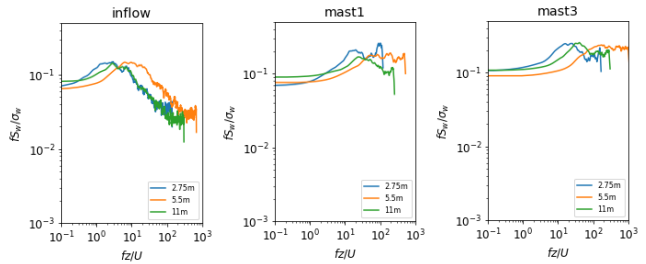

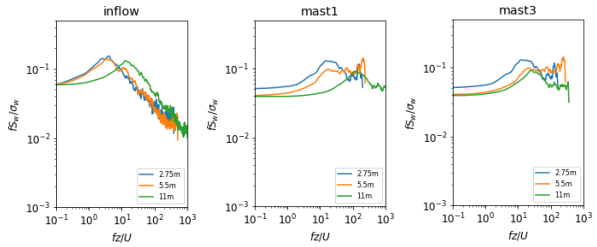

Results – Wind and Turbulence Profiles

- Increased unsteadiness (σ_w) of local flow below the elevation axis height from wake effects of upstream and neighboring **operating heliostats**
- Downward transfer of TKE in the field interior below the elevation axis height for both northerly and southerly wind periods

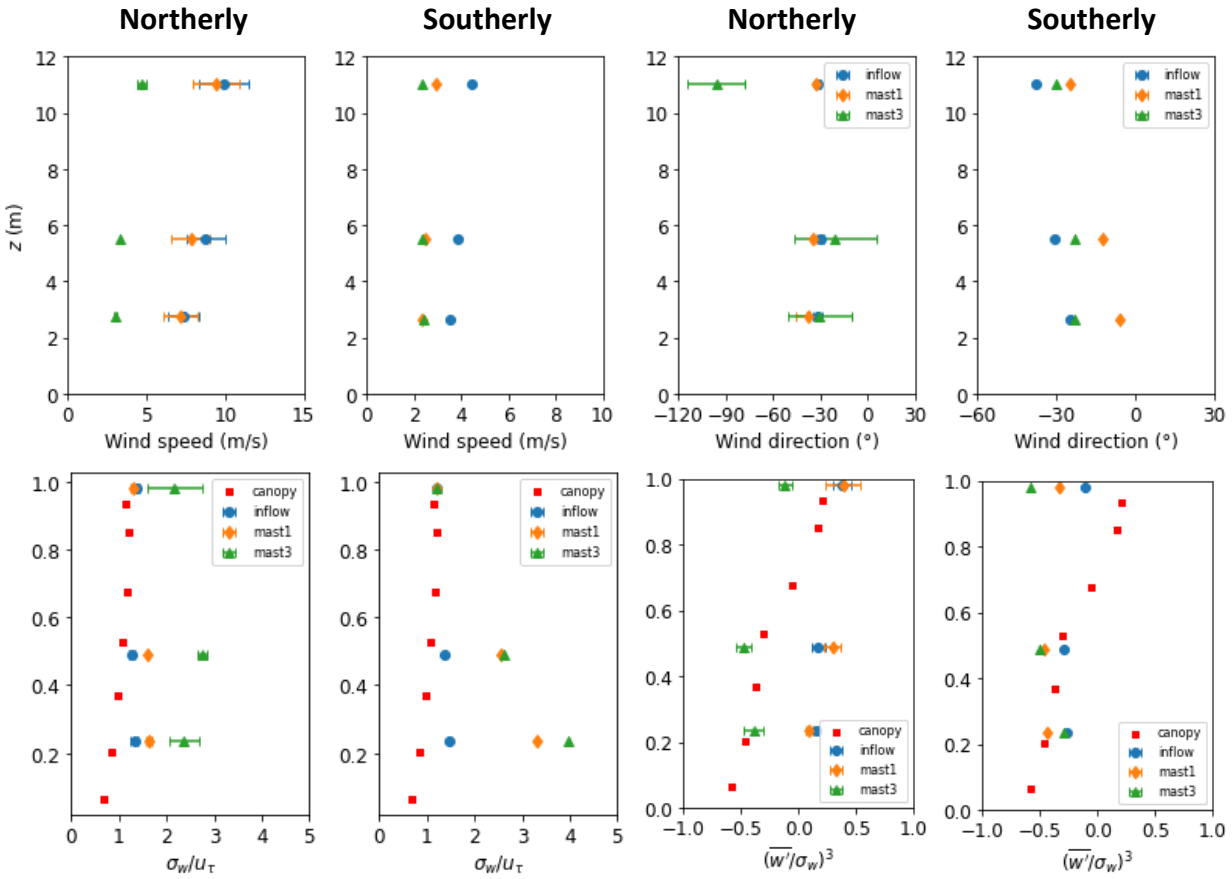

- Increased unsteadiness (σ_w) of local flow at the elevation axis height from wake effects of upstream **stowed heliostats**
- Downward transfer of TKE in the field interior at the elevation axis height for both northerly and southerly wind periods

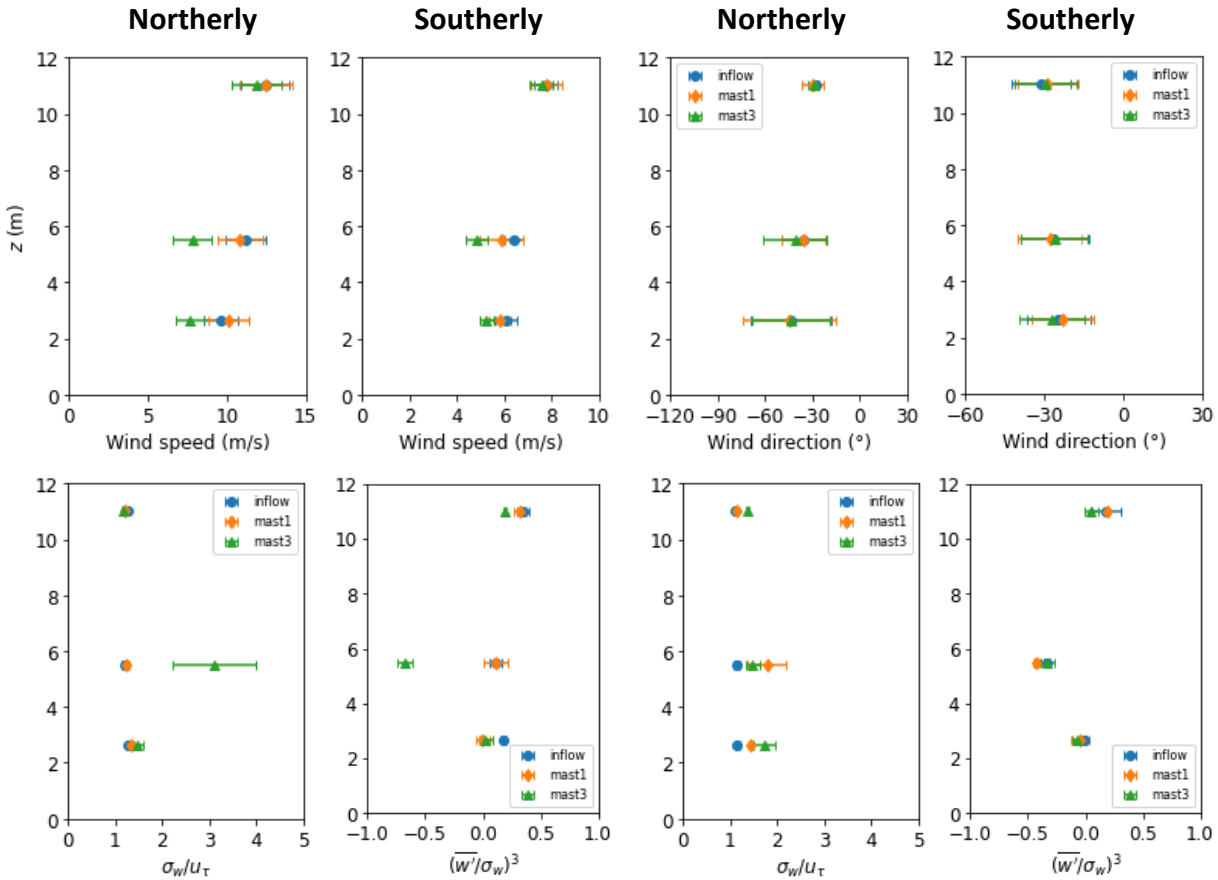

Results – Loads Time Series and Distributions

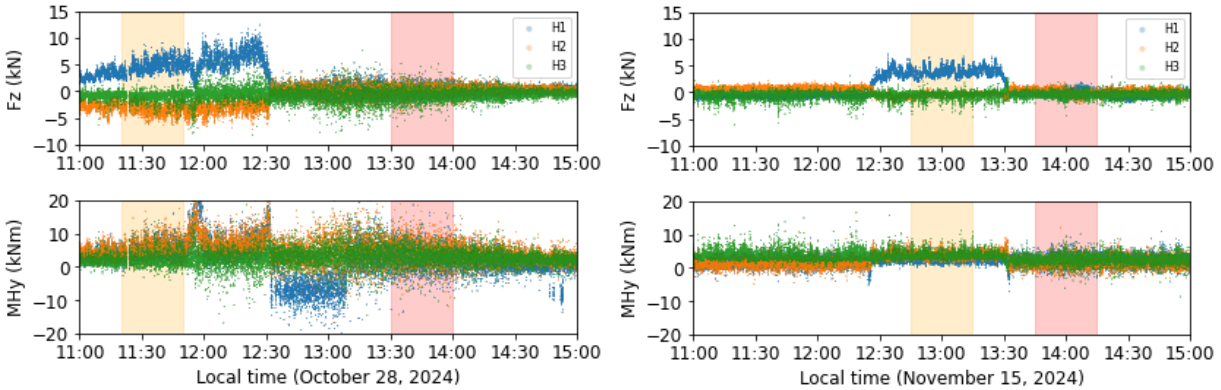

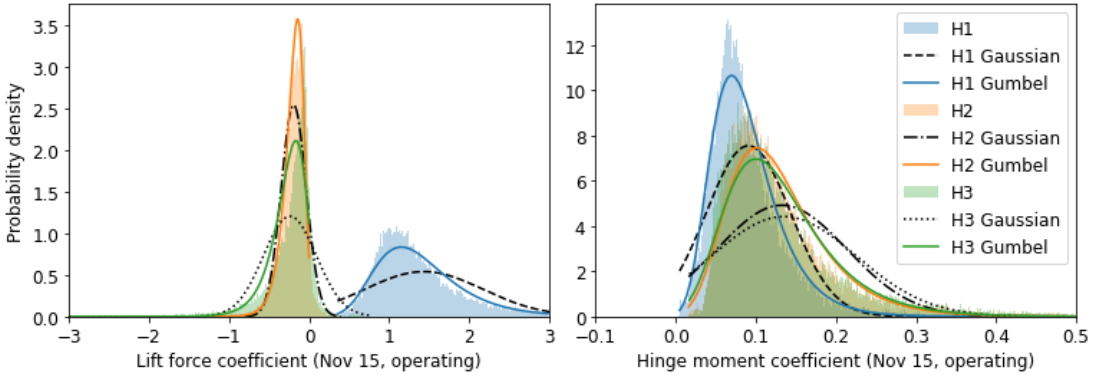

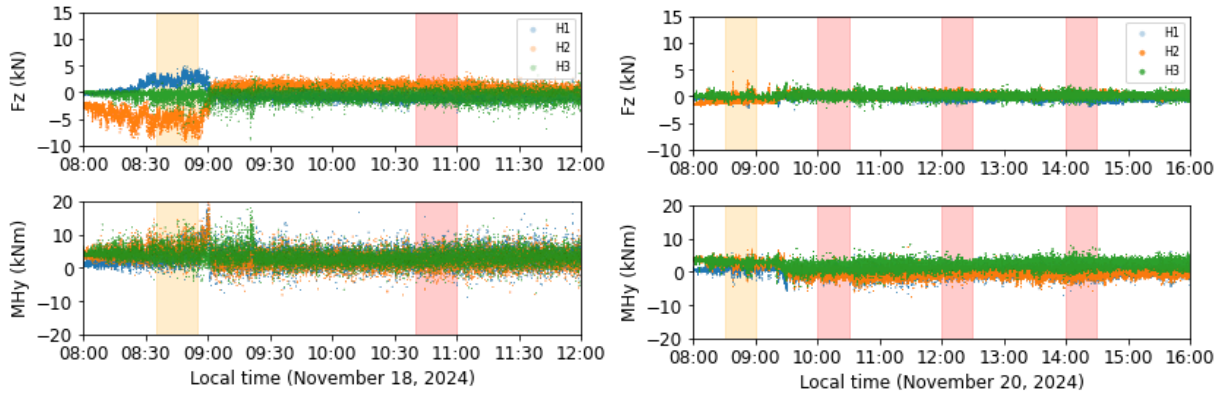

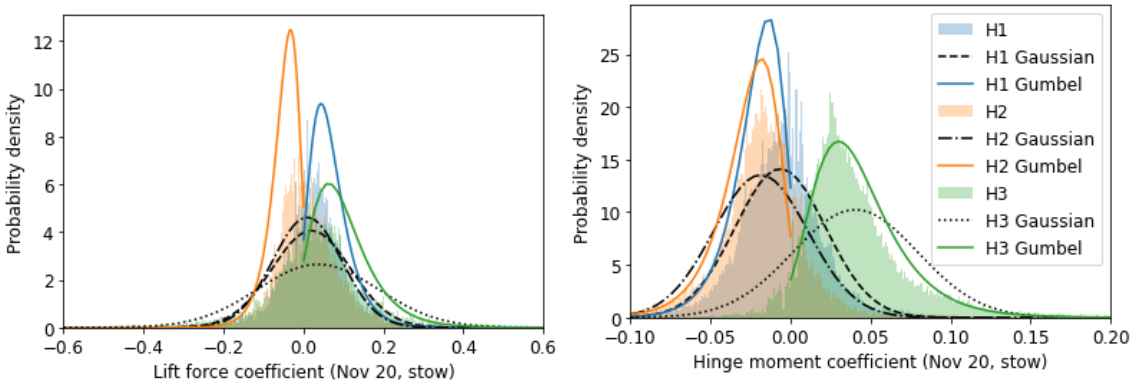

Results – Load Coefficients (Northerly)

Operating (α = 68-69°) and stow (α = 0°) on October 28, 2024

Load coefficients	Lift force		Hinge moment		Azimuth moment		Overturning moments	
	Mean	Peak	Mean	Peak	Mean	Peak	Mean	Peak
H1 operating	0.95	2.33	0.08	0.25	0.03	0.17	-0.56, 0.94	-1.49, 2.38
H2 operating	-0.69	-2.04	0.10	0.32	0.03	0.16	-0.60, 0.94	-1.76, 2.68
H3 operating	-0.22	-1.49	0.04	0.18	0.01	0.14	-0.25, 0.31	-0.97, 1.13
H1 stow	0.003	0.32	0.03	0.14	0.004	0.015	0.02, -0.01	0.21, -0.22
H2 stow	0.005	0.35	0.05	0.18	0.011	0.030	-0.05, 0.16	-0.25, 0.33
H3 stow	-0.10	-0.57	0.03	0.13	-0.001	-0.008	-0.04, 0.05	-0.25, 0.23

Operating (α = 74-76°) and stow (α = 0°) on November 18, 2024

Load coefficients	Lift force		Hinge moment		Azimuth moment		Overturning moments	
	Mean	Peak	Mean	Peak	Mean	Peak	Mean	Peak
H1 operating	0.43	1.06	0.07	0.23	0.009	0.11	-0.76, 0.74	-1.98, 1.90
H2 operating	-0.98	-2.65	0.09	0.28	0.03	0.15	-0.77, 0.81	-2.09, 2.15
H3 operating	-0.15	-0.78	0.07	0.23	-0.005	-0.13	-0.32, 0.27	-1.06, 0.90
H1 stow	-0.11	-0.39	0.03	0.12	0.001	0.009	-0.01, 0.05	-0.14, 0.21
H2 stow	0.15	0.46	0.03	0.11	0.016	0.038	-0.02, 0.06	-0.16, 0.22
H3 stow	-0.10	-0.46	0.04	0.12	0.002	0.010	-0.05, 0.03	-0.21, 0.17

Operating (α = 68-69°) and stow (α = 0°) on November 15, 2024

Load coefficients	Lift force		Hinge moment		Azimuth moment		Overturning moments	
	Mean	Peak	Mean	Peak	Mean	Peak	Mean	Peak
H1 operating	1.43	3.65	0.09	0.25	0.07	0.25	-0.11, 0.89	-0.54, 2.29
H2 operating	-0.19	-0.66	0.13	0.38	0.08	0.27	-0.32, 1.21	-0.95, 3.29
H3 operating	-0.24	-1.23	0.13	0.41	0.05	0.23	-0.13, 0.50	-0.74, 1.71
H1 stow	-0.02	-0.59	0.04	0.16	0.0003	0.05	-0.03, 0.09	-0.21, 0.41
H2 stow	0.07	0.48	0.04	0.17	0.04	0.09	-0.05, 0.12	-0.26, 0.61
H3 stow	-0.09	-0.57	0.05	0.16	0.004	0.03	-0.03, 0.04	-0.20, 0.23

For prevailing **northerly** winds:

- Peak lift force coefficients on **operating** heliostats are largest in magnitude in the prevailing two rows (often second row) at the field edge
- Peak lift force coefficients on **stowed** heliostats are similar in magnitude and can increase in the interior of the field compared to the field edge
- Peak hinge moment coefficients on **operating** heliostats can increase or decrease in magnitude from the field edge to the interior
- Peak hinge moment coefficients on **stowed** heliostats are similar in magnitude from the field edge to the interior
- Peak overturning moment coefficients on **operating** heliostats are largest in magnitude in the second prevailing row and decrease in the interior
- Peak overturning moment coefficients on **stowed** heliostats reduce in magnitude from the field edge to the interior

Results – Load Coefficients (Northerly)

	Load coefficients	Lift force		Hinge moment		Azimuth moment		Overturning moment	
		Mean	Peak	Mean	Peak	Mean	Peak	Mean	Peak
Oct 28, 2024	CD $\beta = 180°$	0.95	2.33	0.08	0.25	0.03	0.17	-0.56, 0.94	-1.49, 2.38
Nov 15, 2024	CD $\beta = 180°$	1.43	3.65	0.09	0.25	0.07	0.25	-0.11, 0.89	-0.54, 2.29
Nov 18, 2024	CD $\beta = 180°$	0.43	1.06	0.07	0.23	0.009	0.11	-0.76, 0.74	-1.98, 1.90
	ABLRF $\beta = 0°$	1.04	1.44	0.20	0.36	0.05	0.25	1.72	3.70
	WT $\beta = 0°$	0.58	1.02	0.05	0.36	0.05	0.43	2.58	1.61, 3.13
	WT $\beta = 180°$		0.29, 0.73		0.11, 0.20		0.11, 0.24		1.22, 1.96

For prevailing **northerly** winds on single **operating** heliostat:

- Peak lift force coefficients are underpredicted in WT and ABLRF compared to CD H1
- Peak hinge moment coefficients are overpredicted in WT and ABLRF compared to CD H1
- Peak azimuth moment coefficients in WT and ABLRF are at the upper bound of CD H1
- Peak overturning moment coefficients are overpredicted in WT and ABLRF compared to CD H1

	Load coefficients	Lift force		Hinge moment		Azimuth moment		Overturning moment	
		Mean	Peak	Mean	Peak	Mean	Peak	Mean	Peak
Oct 28, 2024	CD $\beta = 180°$	0.003	0.32	0.03	0.14	0.004	0.015	0.02, -0.01	0.21, -0.22
Nov 15, 2024	CD $\beta = 180°$	-0.02	-0.59	0.04	0.16	0.0003	0.05	-0.03, 0.09	-0.21, 0.41
Nov 18, 2024	CD $\beta = 180°$	-0.11	-0.39	0.03	0.12	0.001	0.009	-0.01, 0.05	-0.14, 0.21
	ABLRF $\beta = 0°$	0.53	0.84	0.21	0.31	0.004	0.05	0.68	1.04
	WT $\beta = 0°$	0.10	0.60	0.07	0.29	0.007	0.13	0.30	0.25, 0.59
	WT $\beta = 180°$		0.23, 0.65		0.07, 0.12		0.06, 0.13		0.64, 1.30

For prevailing **northerly** winds on single **stowed** heliostat:

- Peak lift force coefficients are overpredicted in WT and ABLRF compared to CD H1
- Peak hinge moment coefficients are overpredicted in WT and ABLRF compared to CD H1
- Peak azimuth moment coefficients in WT are overpredicted and ABLRF similar in magnitude to CD H1
- Peak overturning moment coefficients in WT and ABLRF are overpredicted compared to CD H1

ABLRF and WT $\beta = 0°$ https://doi.org/10.1016/j.solener.2024.112742
WT $\beta = 180°$ https://doi.org/10.52825/solarpaces.v1i.725

$$C_{My} = C_{MHy}(c/H) + C_{Fx}$$

Results – Load Coefficients (Southerly)

Operating (α = 78-80°) and stow (α = 0°) on November 20, 2024

Load coefficients	Lift force		Hinge moment		Azimuth moment		Overturning moments	
	Mean	Peak	Mean	Peak	Mean	Peak	Mean	Peak
H1 operating	-0.98	-3.08	0.18	0.75	0.15	0.75	0.61, -1.52	2.72, -3.49
H2 operating	-1.16	-3.80	0.42	1.16	0.32	1.05	-0.50, 0.46	-3.15, 2.71
H3 operating	-0.01	-2.06	0.41	1.15	0.17	0.85	-0.06, -0.65	-2.68, -2.54
H1 stow	0.03	0.42	-0.01	-0.13	-0.009	-0.04	0.13, -0.09	0.36, -0.55
H2 stow	0.01	0.38	-0.03	-0.15	0.041	0.11	0.05, -0.16	0.24, -0.46
H3 stow	0.05	0.65	0.06	0.23	-0.006	-0.03	-0.09, -0.20	0.38, -0.36

Two stow (α = 0°) periods on November 20, 2024

Load coefficients	Lift force		Hinge moment		Azimuth moment		Overturning moments	
	Mean	Peak	Mean	Peak	Mean	Peak	Mean	Peak
H1 stow1	-0.28	-0.71	0.005	0.11	-0.03	-0.07	0.09, -0.07	0.26, -0.10
H2 stow1	0.36	0.95	0.004	0.11	0.08	0.19	0.08, -0.04	0.26, -0.12
H3 stow1	0.002	0.49	0.16	0.40	-0.01	0.04	0.07, -0.03	0.24, -0.13
H1 stow2	-0.31	-0.81	-0.009	0.12	-0.02	-0.05	0.10, -0.09	0.34, -0.31
H2 stow2	0.56	1.31	0.006	0.12	0.12	0.27	0.08, -0.05	0.30, -0.26
H3 stow2	0.03	0.59	0.13	0.32	0.02	0.05	0.11, -0.02	0.35, -0.21

For **southerly** winds passing through the heliostat field:

- Peak lift force coefficients on **stowed** heliostats are largest in magnitude in the second row (H2) from the field edge and can increase in the interior of the field compared to the field edge
- Peak hinge moment coefficients on **stowed** heliostats increase in magnitude from the field edge to the interior
- Peak overturning moment coefficients on **stowed** heliostats are generally similar in magnitude and can reduce in magnitude from the field edge to the interior

Results – Acceleration Spectra

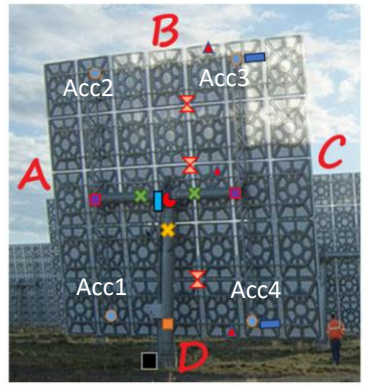

- Peak acceleration spectra frequencies ~1.8 Hz and ~3 Hz during operation and stow
- Lower energy spectral peaks ~8 Hz in operation and ~5 Hz near top edges in operation and all in stow

Peak freq (Hz)	H1 operation	H2 operation	H3 operation	H1 stow	H2 stow	H3 stow
Acc1	1.77 3.04	1.91 3.03	1.83 3.02	1.83 3.02	1.84 3.05	1.76 3.03
Acc2	1.87 3.04	1.91 3.03	1.79 3.04	1.75 3.02	1.84 3.03	1.76 3.02
Acc3	1.78 3.03	1.94 3.05	1.78 3.02	1.83 3.02	1.79 3.05	1.76 3.02
Acc4	1.80 3.04	1.94 3.03	1.74 3.04	1.83 3.02	1.79 3.05	1.89 3.02

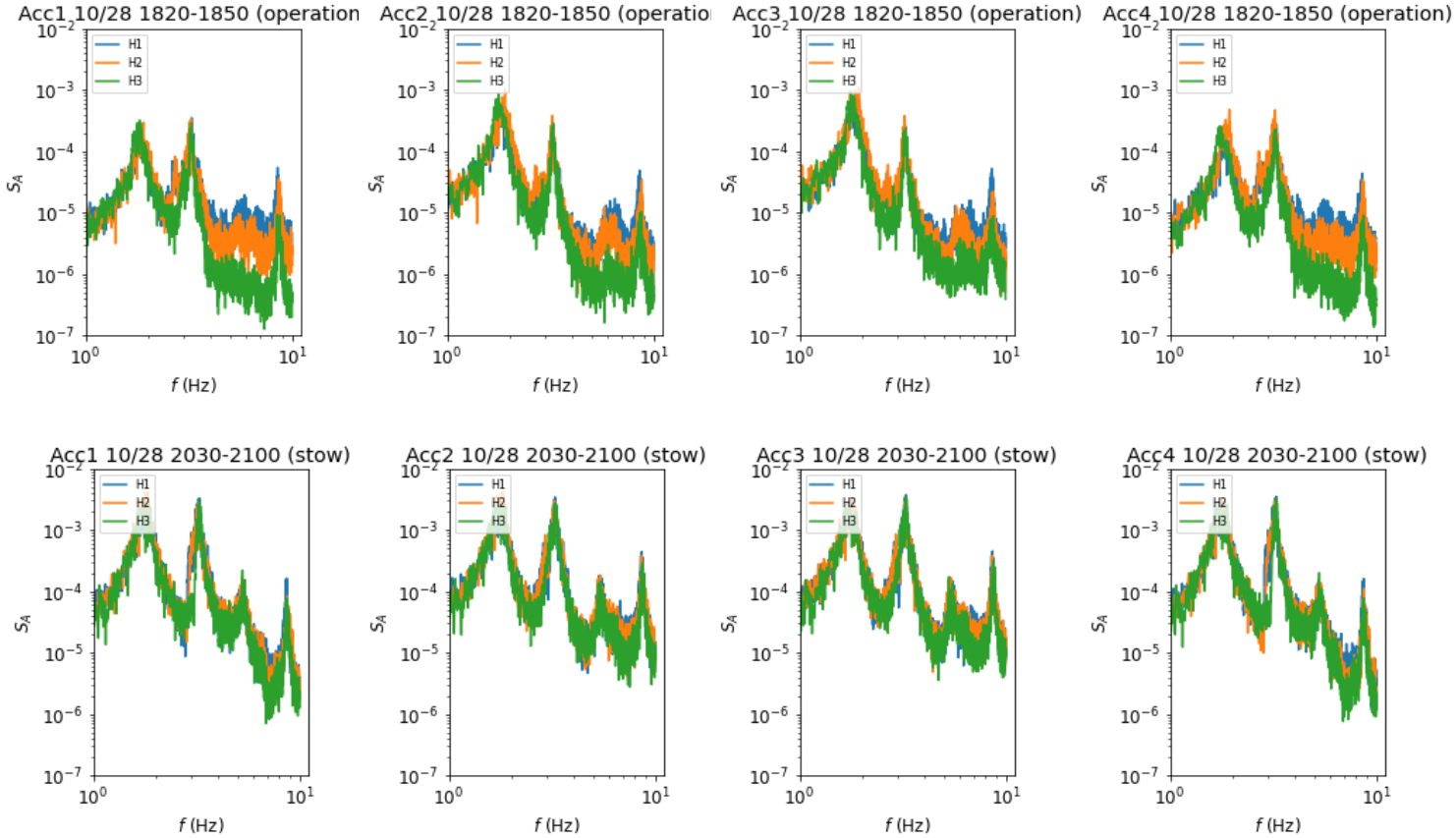

Conclusions and Future Work

- Lift forces and hinge moments decrease in the interior during field operation and can increase in the interior during field stow
- The direction of lift force is reversed (downward) and the magnitude of hinge moment is amplified in the field interior because of wake effects of upstream heliostats and resulting downward transfer of TKE
- Future work to analyze overturning moments, azimuth moments, displacements and accelerations on facet surface for dynamic load analysis

Acknowledgments

This work was authored by the National Laboratory of the Rockies for the U.S. Department of Energy (DOE), operated under Contract No. DE-AC36-08GO28308. Funding provided by U.S. Department of Energy Office of Critical Minerals and Energy Innovation Solar Energy Technologies Office Award DE-EE00052732. The views expressed in the article do not necessarily represent the views of the DOE or the U.S. Government. The U.S. Government retains and the publisher, by accepting the article for publication, acknowledges that the U.S. Government retains a nonexclusive, paid-up, irrevocable, worldwide license to publish or reproduce the published form of this work, or allow others to do so, for U.S. Government purposes.

NLR/PR-5700-101670